Atmospheric Pollution Research 8 (2017) 660–668

Contents lists available at ScienceDirect

Atmospheric Pollution Research

journal homepage: http://www.journals.elsevier.com/locate/apr

ARIMA analysis of the effect of land surface coverage on PM_{10} concentrations in a high-altitude megacity

Carlos Zafra*, Yenifer Ángel, Eliana Torres

Environmental Engineering, Faculty of Environment and Natural Resources, Francisco José de Caldas District University, Av. Circunvalar Venado de Oro, E-111711, Bogotá D.C., Colombia

ARTICLE INFO

Article history:
Received 10 November 2016
Received in revised form
4 January 2017
Accepted 5 January 2017
Available online 12 January 2017

Keywords:
ARIMA
Bogota
Land surface coverage
PM_{10}
Urban air quality

ABSTRACT

This paper uses ARIMA models for daily temporal analysis of the effect of land surface coverage (LSC) on PM_{10} concentrations in a high-altitude megacity. Bogota, the capital of Colombia, is the urban center with the greatest population density and third-highest air pollution levels in Latin America. Six automatic monitoring stations were used; they were equipped with measurement instruments for PM_{10}, temperature and solar radiation as well as wind speed and wind direction. The duration of the sampling period was 6 years. The hourly PM_{10} sampling system included continuous-monitoring equipment that used beta ray attenuation. We analyzed atmospheric stability and the spatial distribution of LSC (vegetated, non-vegetated, impervious and water bodies) before applying the iterative process of Box-Jenkins for ARIMA models. ARIMA analysis indicates greater persistence in PM_{10} pollution in the presence of increased vegetated LSC (trees and grasslands); persistence decreased in the presence of more impervious LSC (roofs, pavements and footpaths). PM_{10} persistence is found to be 2 days (48 h). The best distance to demonstrate these findings is between 50 and 100 m, with respect to the monitoring stations' physical location. Urban areas with a predominance of vegetated LSC register lower PM_{10} concentrations than urban areas with a predominance of impervious LSC (average daily difference = 42.7%). This study's findings serve as a reference point for the development of differentiated strategies for air pollution control in line with urban LSC.

© 2017 Turkish National Committee for Air Pollution Research and Control. Production and hosting by Elsevier B.V. All rights reserved.

1. Introduction

Increased levels of respiratory disease in children and older adults caused by air pollution in urban areas is strongly correlated with increased levels of atmospheric particulate matter (Pope and Dockery, 2006; Chow et al., 2006; Wang et al., 2015). Higher levels of particulate matter (PM) are mainly associated with the concentration of industrial activities and quantity of motor vehicles in urban areas (Jian et al., 2012; Soto et al., 2014; Gocheva-Ilieva et al., 2014). Thus, many countries have decided to enhance active monitoring in urban areas to control this atmospheric pollutant. In consequence, the study of a possible relationship between PM concentrations and type of land surface coverage (LSC) in urban areas becomes urgent from a public health perspective. Climate conditions of the study area cannot be ignored for this type of analysis (Connell et al., 2005; Díaz-Robles et al., 2008). Zhang et al. (2012) and Seinfeld and Pandis (2016) reported that the distribution and transport of PM depended significantly on the condition of atmospheric stability (AS) and LSC (i.e., existing land use).

Studies in urban areas have reported a significant influence of LSC on PM_{10} concentrations. Chen et al. (2015) found that the presence of trees in Wuhan (China) reduced PM_{10} concentrations between 7 and 15%. Similarly, Islam et al. (2012) and Yin et al. (2007) reported a reduction of total suspended particulates (<100 μm) in urban areas by 55% (Khulna, Bangladesh) and 30% (Shanghai, China), respectively. McDonald et al. (2007) used GIS techniques, along with field research, to forecast an increase between 3.7 and 16.5% and 3.6 and 8.0% of the total tree coverage in conurbations of West Midlands and Glasgow (United Kingdom) would generate a reduction of 10% and 2% in primary PM_{10} concentrations, respectively. LSC with trees acts as an effective sink of

* Corresponding author.
E-mail addresses: czafra@udistrital.edu.co (C. Zafra), ykangell@udistrital.edu.co (Y. Ángel), eytorresp@udistrital.edu.co (E. Torres).

Peer review under responsibility of Turkish National Committee for Air Pollution Research and Control.

http://dx.doi.org/10.1016/j.apr.2017.01.002
1309-1042/© 2017 Turkish National Committee for Air Pollution Research and Control. Production and hosting by Elsevier B.V. All rights reserved.

gaseous and particulate atmospheric pollutants (Gallagher et al., 2002; Fowler et al., 2004). However, the mineral dust emanating from bare land was identified as the source of decreased air quality in several cities in Central Europe (e.g., Berlin and Zurich) (Wolf-Benning et al., 2009; Minguillon et al., 2012). Titos et al. (2014) reported that during dry summer conditions, more than 50% of PM_{10} corresponded to mineral dust re-suspended from bare soils and urban roads in Granada (Spain). Waked et al. (2014) found that 13% of average annual PM_{10} from Lens (France) could be traced to bare soils (mineral dust sources). Researchers have reached consensus on the main parameters that determine the dust and PM_{10} production, namely the saltation rate (kinetic energy by wind) and soil texture (Avecilla et al., 2016). Several authors found that the potential PM_{10} emissions increased as a function of silt and clay content decreased as a function of the soil's sand content (e.g., Carvacho et al., 2004; Funk et al., 2008). Liu et al. (2016) compared the removal efficiency of PM at different underlying surfaces in Beijing (China). The authors' results showed that urban forest surface had the best removal capacity because of its relatively low re-suspension rate. The PM removal efficiency of water bodies was higher than that of bare land due to the relatively higher PM re-suspension rates of bare land.

Studies show that AS plays an important role in the transport and dispersion of PM_{10}; it is significantly correlated to variations of temperature in altitude and wind speed (Zoras et al., 2006; Perrino et al., 2008; Chambers et al., 2015). Lee et al. (2013) indicated that, in the presence of extreme AS conditions (thermal inversion) in Seoul (South Korea), PM_{10} concentrations increased significantly (>100 $\mu g/m^3$). Vecchi et al. (2007) reported a 13% increase in PM_{10} concentrations under the prevailing conditions of nocturnal AS in Milan (Italy), despite a reduction in the active emission sources such as traffic, domestic heating and industrial activity. Under daytime conditions of atmospheric instability, PM_{10} concentrations tend to decrease (greater dispersion).

Air quality modeling has shown that more sophisticated multi-parametric meteorological models tend to significantly underestimate or overestimate air pollutant concentrations due to the complexity of phenomena involved (e.g., Argiriou, 2007; Kumar and Jain, 2010; Zhang et al., 2013; Seinfeld and Pandis, 2016). This complexity is due to the physicochemical processes undergone by pollutants, weather conditions, LSC, and uncertainty in the information of parameters in study. Thus, short- and long-term forecasts can be based on the statistical modeling of time series (Díaz-Robles et al., 2008; Kumar and Jain, 2010; Reisen et al., 2014). Athanasiadis et al. (2005) compared several statistical models (linear regression analysis-LRA, auto-regressive integrated moving average-ARIMA and principal components analysis-PCA) and classification algorithms (artificial neural networks, decision trees and conjunctive rules); the authors arrived at the conclusion that, in terms of the root-mean-square error, linear regression (0.128), and ARIMA (0.153) models were the most suitable for modeling urban air quality. ARIMA models developed for the statistical analysis of time series have been applied in several studies; these studies have reported a reasonable adjustment and utility for simulating and forecasting the behavior of atmospheric pollutants (e.g., Liu, 2009; Gocheva-Ilieva et al., 2014; Soni et al., 2014). ARIMA models have been deemed useful for assessing the temporal persistence of atmospheric pollutants have been reported (e.g., Turias et al., 2008; Kumar and De Ridder, 2010). For the sake of clarity, persistence refers to the continuation of a pollutant concentration pattern from one period to the next (Meraz et al., 2015). Specifically, these models provided an auto-regressive method ("memory" of the phenomenon) for interpreting data variability in time series for atmospheric pollutants (Hernández et al., 1992; Díaz-Robles et al., 2008; Hsu et al., 2014).

This study was done using data from a Latin-American megacity (8.85 million inhabitants in 2015). Bogota (Colombia) is a high-altitude city located in the Andes Mountains (04°36′35″ N, 74°04′54″ W); its average altitude is 2600 masl. The city's tropical mountain climate is characterized by large hourly temperature variations (maximum variation = 12 °C). The city is recognized as the urban center with the greatest population density (26,000 inhabitants/km^2) and third highest air pollution level in Latin America (Nelson et al., 2005; Sarmiento et al., 2015). In global terms, there have been few published studies that evaluate the behavior of PM_{10} in the urban centers of developing countries with similar physical characteristics and climate conditions; this lack of research has, in part, driven the development of this study.

This article used ARIMA models for the daily temporal analysis (2007–2012) of the influence of LSC on PM_{10} concentrations in a high-altitude megacity. The study was conducted using six automatic monitoring stations located in four zones in Bogota: Kennedy, Puente Aranda, Suba and Barrios Unidos. The monitoring stations used herein cover 23.9 km of the city's urban area.

2. Materials and methods

2.1. Research site description

Six automatic monitoring stations were placed in the localities of Kennedy (S1 and S2), Puente Aranda (S3), Suba (S4 and S5), and Barrios Unidos (S6) in Bogota, Colombia (see Fig. 1). The tropical mountain climate (cold weather) of the study sites had an average daily temperature (during the sampling period) between 13.3 and 14.3 °C, with hourly variations between 7.2 and 19 °C. Table 1 shows the main characteristics of the areas covered by each monitoring station. All six stations were equipped with PM_{10} measuring devices, in addition to devices to measure temperature, wind speed, and wind direction. S1, S5, and S6 stations were further equipped with instruments used to measure solar radiation. The monitoring stations covered a total of 23.9 km of the city's urban area (Fig. 1). The altitude of the monitoring stations was close to that of Bogota, between 2563 and 2590 masl.

2.2. PM_{10} sampling system

The sampling period lasted 6 years (01/01/2007-12/31/2012). The hourly PM_{10} sampling system consisted of continuous-monitoring equipment using beta ray attenuation (Met One Instruments, BAM 1020). The sampling protocol followed the guidelines set forth by the United States Environmental Protection Agency in EPA/625/R-96/010a-IO-1.2 (U.S.EPA, 1999). The equipment's constant flow rate was 16.7 l/min. The lowest detection limit was 3.6 $\mu g/m^3$ and 1.0 $\mu g/m^3$ for hourly and daily sampling intervals, respectively. Resolution in the measurement was 0.24 μg in a range of 1 mg. The precision was ±8% for hourly intervals and ±2% for daily intervals.

2.3. Atmospheric stability analysis

AS in the study areas was determined through the methodologies established by Pasquill (1961), Turner (1964) and Gifford (1976), with hourly data for wind speed and solar radiation (Zoras et al., 2006; Chambers et al., 2015). The predominant AS condition, measured as hourly occurrence frequency in the urban area covered by the monitoring stations (23.9 km of distance), was analyzed. Monitoring stations used for this calculation were S1, S5, and S6 (see Fig. 1). A Kruskal-Wallis test to assess the differences in hourly occurrence frequency between monitoring stations was applied (df = 24, per monitoring station). This is a non-parametric

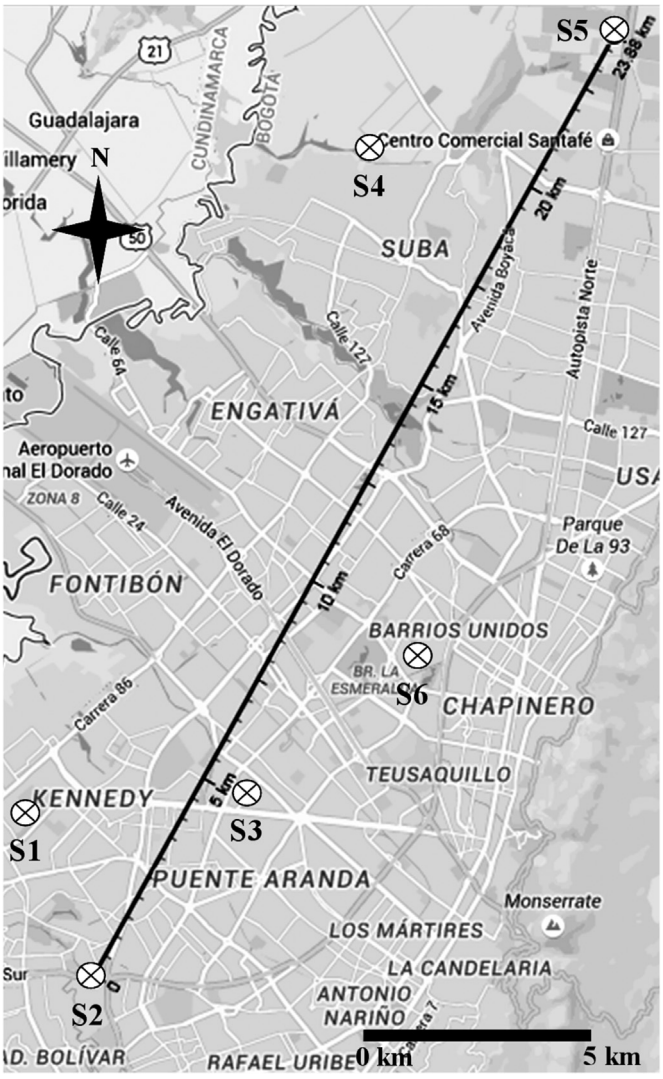

Fig. 1. Location of monitoring stations in Bogota, Colombia (Google Maps, 2015). S1-Kennedy, S2-Carvajal, S3-Puente Aranda, S4-Corpas, S5-Guaymaral, and S6-Barrios Unidos.

alternative to a one-way ANOVA. The non-normal distribution of AS data was determined with Shapiro-Wilk test (df = 24; *p*-values < 0.001). The following quantitative scale was used to identify each AS condition: 1 = stable, 2 = slightly stable, 3 = neutral, 3.5 = neutral to slightly unstable, 4 = slightly unstable, 4.5 = slightly unstable to unstable, 5 = unstable, 5.5 = unstable to very unstable, and 6 = very unstable. This quantitative scale was developed to graphically represent hourly variations in AS.

2.4. Land surface coverage analysis

To determine the type of LSC around each monitoring station, we drew on satellite images (DigitalGlobe's QuickBird satellite, 2.0-m resolution), making an initial box of 80,000 m^2, with diagonals of 400 m, and a center for each monitoring station. Additionally, to assess the spatial variation per LSC type, boxes of different lengths in terms of diagonals were considered for each monitoring station: 100 m (5000 m^2), 200 m (20,000 m^2), 400 m (80,000 m^2), 800 m (320,000 m^2), 1600 m (1,280,000 m^2) and 3200 m (10,240,000 m^2). Previous studies have relied on land use and air quality, respectively, as methodological guides (e.g., Bach et al., 2015; Irga et al., 2015). In this study, four types of LSC were considered: vegetated (trees and grasslands), non-vegetated (bare soil), impervious (roofs, pavements and footpaths) and water bodies (rivers, lakes, and wetlands). In the selected monitoring stations, there was no LSC variation during the PM_{10} monitoring period.

2.5. PM_{10} data analysis

Hourly variation in the PM_{10} concentrations for all monitoring stations was evaluated from average values for the entire study period (n = 24, per monitoring station). An analysis with the Spearman's correlation coefficient (*rs*) to assess relations in the average hourly PM_{10} concentration between monitoring stations was carried out. The non-normal distribution of PM_{10} data was determined with Shapiro-Wilk test (df = 24; *p*-values < 0.048). A graphical comparison between the hourly variation of the average PM_{10} concentration and average AS condition was carried out to study the influence of the hourly cycles of PM_{10} emission from motor vehicles and industries located across the entire study area. Finally, the average daily PM_{10} concentrations of monitoring stations located in areas with predominantly impervious LSC (S1, S2, and S3) were compared with the concentrations of stations located in areas with predominately vegetated LSC (S4, S5, and S6).

Table 1
Characteristics of the location areas of monitoring stations.

Characteristics	S1 (Kennedy)	S2 (Carvajal)	S3 (Puente Aranda)	S4 (Corpas)	S5 (Guaymaral)	S6 (Barrios Unidos)
Coordinates	4°37′30.18″N 74°9′40.80″W	4°35′44.22″N 74°8′54.90″W	4°37′54.36″N 74°7′2.94″W	4°45′40.49″N 74°5′36.46″W	4°47′1.52″N 74°2′39.06″W	4°39′30.48″N 74°5′2.28″W
Altitude (masl)	2580	2563	2590	2571	2580	2577
Average daily PM_{10} ($\mu g/m^3$)[a]	85.9	81.7	65.7	58.7	34.9	40.0
Average annual rainfall (mm)[a]	521	728	909	762	832	1084
Average daily wind speed[a]	2.2	2.0	2.5	1,2	1.0	1.35
Prevailing wind direction[a]	SW	SW	W	SE	SE	W
Average daily temperature (°C)[a]	14.3	14.3	14.1	13.3	14.2	14.3
Type of zone	Urban	Urban	Urban	Suburban	Suburban	Urban
Land use[b]	R-C	I-R	I-C	R-IN	IN	R-IN
Impervious/Vegetated/Non-vegetated/Water body (%)	68.9/30.7/0.4/0.0	88.2/10.1/0.0/1.7	86.0/4.6/9.5/0.0	35.6/59.7/4.7/0.0	22.6/74.6/1.1/1.7	9.7/86.2/4.1/0.0
PM_{10} sampler location (m)[c]	7	6	13	9	4	4.6
Population density (inhabitant/ha)	400	350	250	150	< 1	30

Note.
[a] During the study period.
[b] R-residential, I-industrial, C-commercial, IN-institutional.
[c] With respect to the land surface.

2.6. ARIMA model development and analysis

Hourly PM_{10} information was added to the ARIMA analysis each day (24-h moving average). The methodology for the development of ARIMA models was based on that of the air quality studies done by Díaz-Robles et al. (2008), Jian et al. (2012), Zhou et al. (2014), and Taneja et al. (2016). We applied the phases of the iterative process of Box and Jenkins (1970) for ARIMA models: identification, parameter estimation, assumption verification, and model use; these phases were developed using the statistical software IBM-SPSS (Statistical Package for the Social Sciences, V. 21.0.0).

The first phase was the identification of a suitable Box-Jenkins model. In this phase, the stationarity of the time series was also determined. To obtain a stationary time series, natural log transformation and differencing process were employed till the seasonality in data fades away. The AR and MA terms of stationary time series data were then obtained by examining the patterns of autocorrelation function (ACF) and partial autocorrelation functions (PACF) plots, which involved much trial and error. Once tentative models were identified, the next phase was parameter estimation of the model. Atypical data for the ARIMA models developed were not considered. This was followed by the assumption verification phase to confirm the adequacy of the identified models in order to select the best fit model.

The appropriateness of the modeling was assessed by the Ljung-Box statistic. This is also known as the modified Box-Pierce statistic. The goodness-of-fit of each model was assessed by the R-squared value (the coefficient of determination). The Ljung-Box statistic tests the null hypothesis of no remaining significant autocorrelation in the residuals of the model and provides an indication of whether the model is correctly specified. A p-value greater than 0.05 implies that the model is correctly specified to describe the correlation information in time series (Ljung and Box, 1978). Other index used to identify the best model was the Bayesian Information Criterion (BIC) (Schwarz, 1978). The optimal model was selected when the BIC was the lowest. A residual analysis was carried out after the modeling to ensure the normality of the residual and no remaining autocorrelations or partial autocorrelations were found. At last, the best fit model was utilized in establishing the time series forecasting values.

The temporary structure of the ARIMA models was analyzed with respect to the spatial variation of LSC, according to the distances of influence established for each monitoring station: 50 m, 100 m, 200 m, 400 m, 800 m, and 1600 m. An analysis with the Spearman's correlation coefficient (rs) to assess relations between LSC types and distances of influence for the monitoring stations with predominantly impervious LSC (S1, S2, and S3) was carried out. The non-normal distribution of data was determined with Shapiro-Wilk test (df = 12; p-values < 0.002). This analysis allowed us to identify the monitoring station and distance of influence appropriate to analyze the possible differences among selected ARIMA models. The previous procedure was also applied for the monitoring stations with predominantly vegetated LSC (S4, S5, and S6): Shapiro-Wilk test, df = 12, p-values < 0.021. Finally, we studied the order of magnitude of the AR and MA terms in relation to the persistence and variability in the time of daily PM_{10} concentrations (Kumar and De Ridder, 2010; Hsu et al., 2014), respectively.

3. Results and discussion

3.1. Atmospheric stability

Fig. 2 shows the average hourly AS condition during the sampling period from the quantitative scale used in this study. The prevailing AS condition between 6 and 18 h (day) was slightly unstable (AS = 4; occurrence frequency for 24 h, f-24 h = 19.5%), unstable (AS = 5; f-24 h = 24.5%), and unstable (AS = 5; f-24 h = 22.7%) for stations S1, S5, and S6, respectively. As for the prevailing AS condition between 18 and 6 h (night) was stable (AS = 1): 35.0% (f-24 h), 49.2% (f-24 h) and 50.0% (f-24 h), respectively. Given the location of the monitoring stations, we deemed stations S2 and S3 to be encompassed by data from station S1, and station S4 to be covered by data from station S5 (see Fig. 1). Therefore, for the entire study area, results indicated that the prevailing AS condition during the day (6–18 h) was slightly unstable and unstable (AS between 4 and 5.5; f-24 h = 46.1%). At night (18-6 h), the prevailing AS condition was stable (AS = 1; f-24 h = 45.1%). Montoya et al. (2004) reported a similar hourly trend for day and night variations of AS in Bogota.

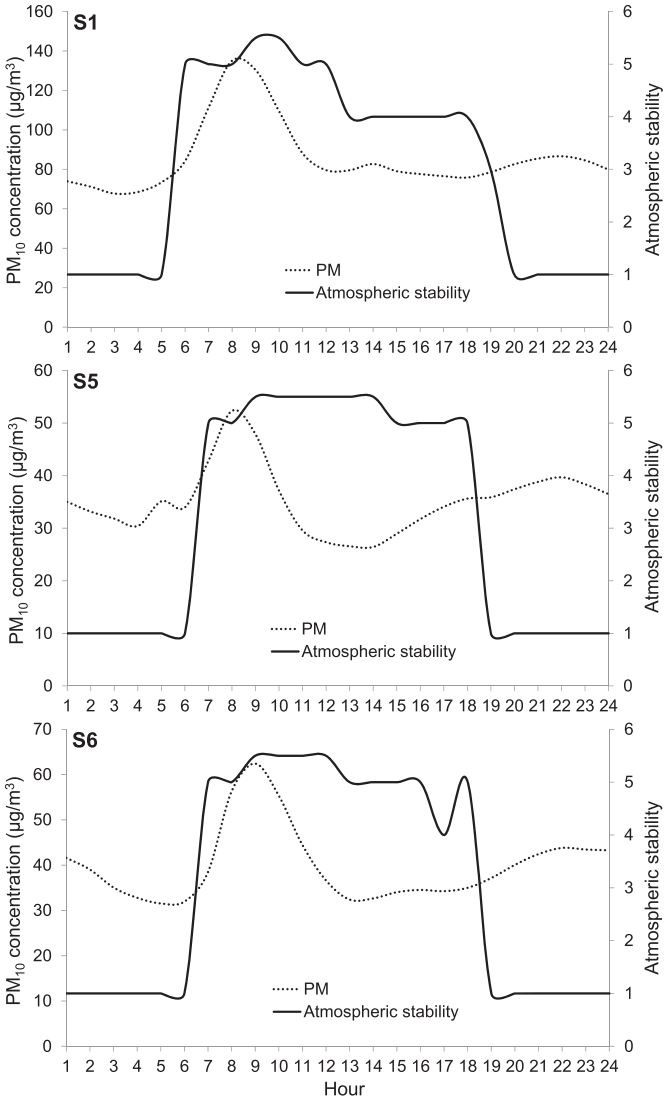

Fig. 2. Average hourly AS condition in the study area (measured values). AS: 1 = stable, 2 = slightly stable, 3 = neutral, 3.5 = neutral to slightly unstable, 4 = slightly unstable, 4.5 = slightly unstable to unstable, 5 = unstable, 5.5 = unstable to very unstable, and 6 = very unstable. PM: Average hourly PM_{10} concentration (measured values).

Additionally, a Kruskal-Wallis test for stations S1, S5, and S6 showed that there were no significant hourly variations in AS (p-value = 0.827). In other words, there was similar behavior in AS for all monitoring stations selected, suggesting that the differences between stations in terms of the ARIMA models developed were not significantly influenced by AS (for this study).

3.2. Land surface coverage

Fig. 3 shows the variation in the LSC type for the distances of influence for each monitoring station. Three monitoring stations exhibited predominantly impervious LSC: S1, S2, and S3. This type of LSC represented between 54.5 and 85.8%, 80.9 and 93.3%, and 86.0 and 92.0% of the area covered by each monitoring station, respectively, when using the distance of influence established for each monitoring station (between 50 and 1600 m). The precedence order for this LSC in the monitoring stations was S3 > S2 > S1.

However, the three other monitoring stations exhibited predominantly vegetated LSC: S4, S5, and S6. This type of LSC represented between 6.4 and 71.8%, 40.1 and 78.4%, and 39.3 and 97.0% of the area covered by each monitoring station, respectively (Fig. 3). The precedence order for this LSC in the monitoring stations was S6 > S5 > S4. As noted, for ARIMA model-based analysis, there were three monitoring stations with mostly impervious LSC (S1, S2, and S3) and three stations with mostly vegetated LSC (S4, S5, and S6).

3.3. PM_{10} concentration assessment

For all monitoring stations, an increase in the average hourly PM_{10} concentration was observed at 5 a.m. and a decrease was observed between 11 a.m. and noon (12:00 h). Peaks in the PM_{10} concentrations were observed between 8 and 9 a.m. These peaks in PM_{10} concentrations coincided with heaviest traffic intensity in Bogota, which precedes the commencement of standard work activities. Results, on average, showed a similar trend in the hourly PM_{10} concentrations for all monitoring stations during the study period (see Fig. 4a). A Spearman's correlation analysis for all monitoring stations showed positive relationships ranging from medium to very strong, Spearman's *rs* between 0.471 and 0.886 (see Table 2). Hence, these results suggest uniform behavior in the hourly cycles of PM_{10} emission from motor vehicles and industries located across the entire study area. This same behavior was observed for the time series of daily PM_{10} concentrations generated in this study (24-h moving average). Gomišček et al. (2004) and Bathmanabhan and Saragur Madanayak (2010) have reported a similar trend in the hourly cycles of PM_{10} registered by monitoring stations in urban areas of Austria and India, respectively.

In this study, the findings also suggest that the hourly behavior of the PM_{10} concentrations was primarily influenced by the uniform emission cycles of mobile (motor vehicles) and stationary (industries) sources in the study areas, as opposed to being influenced by existing AS condition in Bogota (see Fig. 2). This evinced by the fact that the hourly AS condition during the study period did

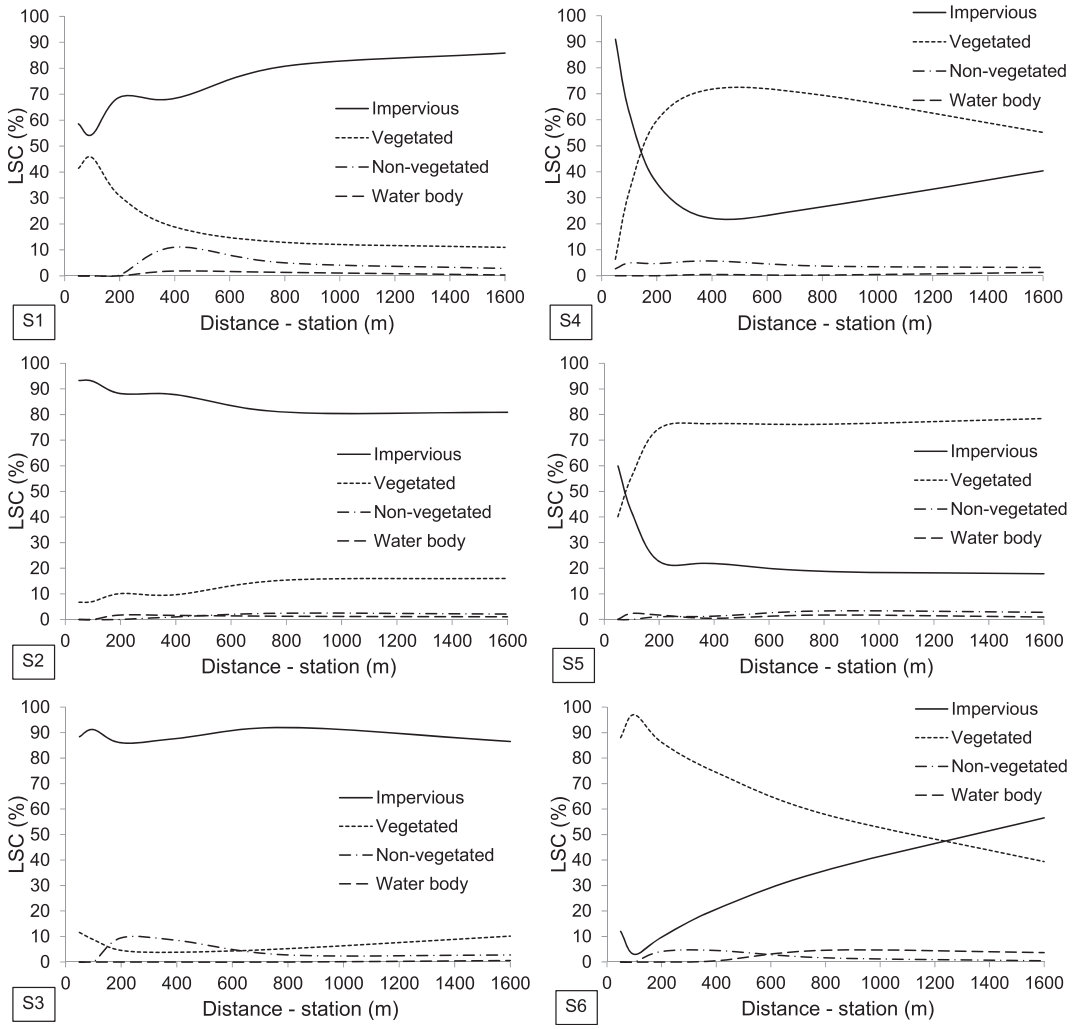

Fig. 3. Spatial variation of the LSC type with respect to the monitoring stations (measured values). Vegetated: trees and grasslands; non-vegetated: bare soil; impervious: roofs, pavements and footpaths; water body: rivers, lakes and wetlands. S1, S2, and S3: predominance of impervious LSC; S4, S5, and S6: predominance of vegetated LSC.

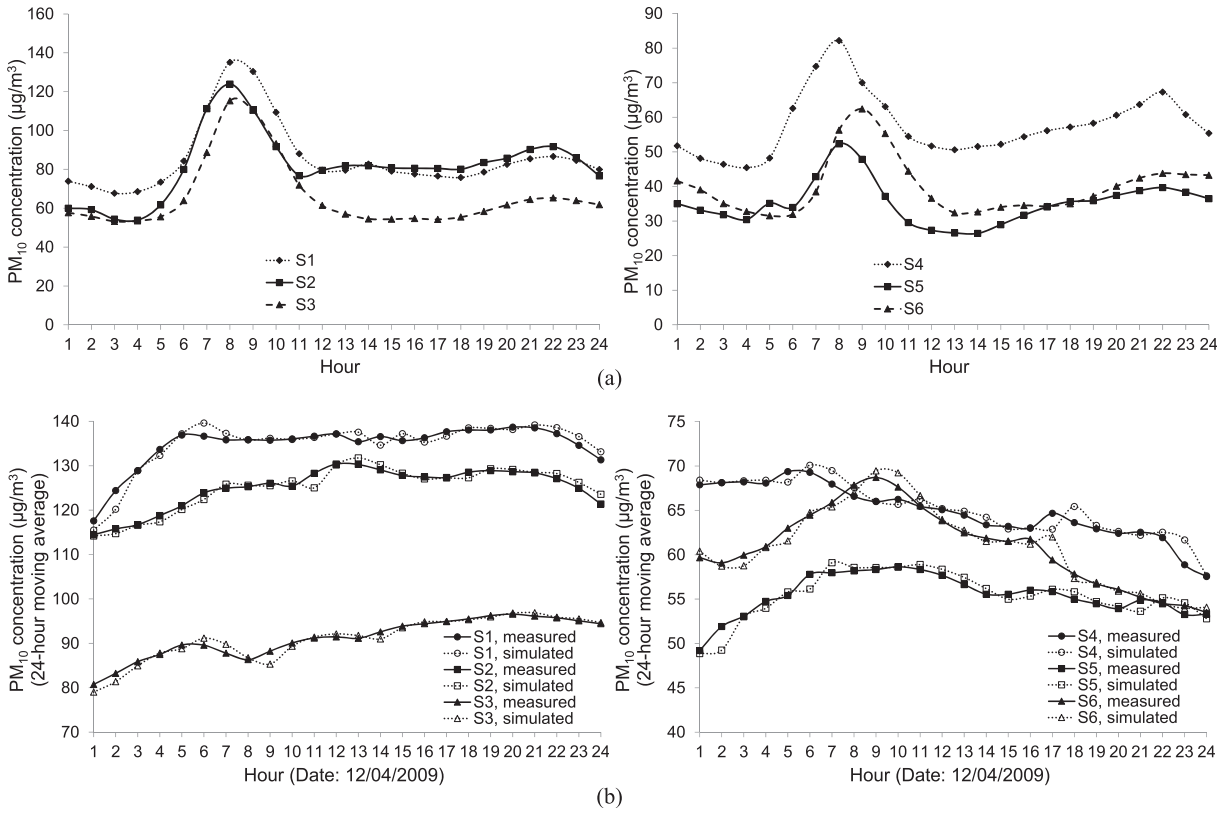

Fig. 4. (a) Average hourly PM_{10} concentration during the entire study period (measured values). (b) PM_{10} concentration, 24-h moving average (measured and simulated values for 12/04/2009). S1, S2, and S3: predominance of impervious LSC. S4, S5, and S6: predominance of vegetated LSC.

Table 2
Spearman's correlations between monitoring stations for the average hourly PM_{10} concentration (n = 24).

Station	S1	S2	S3	S4	S5	S6
S1	1.000					
S2	0.815 (<0.001)[a]	1.000				
S3	0.886 (<0.001)	0.673 (<0.001)	1.000			
S4	0.827 (<0.001)	0.843 (<0.001)	0.807 (<0.001)	1.000		
S5	0.541 (0.006)	0.638 (0.001)	0.691 (<0.001)	0.821 (<0.001)	1.000	
S6	0.620 (0.001)	0.471 (0.020)	0.761 (<0.001)	0.608 (0.002)	0.665 (<0.001)	1.000

Note. [a]*p*-values in parentheses.

not experience significant variations between monitoring stations selected (Kruskal-Wallis test, *p*-value = 0.827). On average, the prevailing AS condition during the day (6 and 18 h) was slightly unstable and unstable (occurrence frequency for 12 h, f-12 h = 92.2%), and at night (18 and 6 h), the prevailing AS condition was stable (EA = 1; f-12 h = 90.2%), which indicates similar behavior in AS for all selected monitoring stations, which suggests that, in the context of this study, the differences between stations in the ARIMA models' terms were not primarily influenced by the AS condition.

Monitoring stations in areas with predominantly vegetated LSC registered lower PM_{10} concentrations than stations in areas with predominantly impervious LSC (see Fig. 4a). As expected, study areas with more vegetated LSC were linked to lower traffic intensity and industrial activity, which likely reduced daily PM_{10} concentrations (average daily reduction = −42.7%). Sun et al. (2016) reported a similar trend in PM_{10} concentrations from an analysis of land use and surface coverage with Moderate-resolution Imaging Spectroradiometer (MODIS) in urban areas of China.

3.4. Development and analysis of ARIMA models

Table 3 shows the terms (AR, I, and MA), model constant, type of transformation, R^2, root-mean-square error, mean absolute percentage error, Ljung-Box Q(18) statistic and *p*-value, and normalized Bayesian information criterion of the ARIMA models developed for PM_{10}. The table also presents the distribution of LSC types according to the distances of influence selected for each monitoring station. Additionally, Table 4 shows the parameter estimates for the ARIMA model terms selected for PM_{10}.

A Spearman's correlation analysis between LSC types and distances of influence for the monitoring stations with predominantly impervious LSC (S1, S2, and S3) showed that the monitoring station with the best correlations on average was S1 (40.7% of significant correlations, *p*-values < 0.05). Additionally, the correlation analysis allowed us to determine the distances of influence for each monitoring station with the best and worst correlations to be 1600 m (44.4% of significant correlations, *p*-values < 0.05) and 100 m (33.3% of significant correlations, *p*-values < 0.05), respectively. These

Table 3
ARIMA models developed for PM_{10} according to the LSC variation in monitoring stations.

Monitoring Station	AR	I	MA	ARIMA model							LSC[a] (%)							
				Constant[b]	Transformation	R^2	RMSE[c]	MAPE[d]	Ljung–Box Q(18), df	*p*-value (Q)	BIC[e]	Distance: 100 m				Distance: 1600 m			
												V	NV	I	WB	V	NV	I	WB
S1	2	1	2	N.C.	Natural log	0.993	2.887	1.076	14.34, 14	0.425	2.121	45.5	0	54.5	0	10.9	2.9	85.9	0.3
	1	1	1	N.C.	Natural log	0.993	2.888	1.081	102.61,16	0.000	2.122								
	1	1	0	N.C.	Natural log	0.993	2.913	1.110	1923.75,17	0.000	2.138								
S2	1	1	0	N.C.	Natural log	0.969	5.514	1.497	17.77, 17	0.404	3.415	7.0	0	93.0	0	16.0	2.1	80.9	1.0
	1	1	1	N.C.	Natural log	0.968	5.516	1.499	2.33, 16	1.000	3.417								
	2	1	2	N.C.	Natural log	0.968	5.477	1.785	39.54,14	0.000	3.402								
S3	1	1	1	N.C.	Natural log	0.971	4.437	1.836	2.47, 16	1.000	2.980	8.8	0	91.2	0	18.2	2.8	86.5	0.5
	1	1	0	N.C.	Natural log	0.971	4.437	1.837	30.60, 17	0.998	2.980								
	2	1	2	N.C.	Natural log	0.970	4.439	1.838	3.40,14	0.022	2.983								
												Distance: 50 m				**Distance: 800 m**			
S4	1	1	3	N.C.	Natural log	0.999	0.741	0.768	14.80, 14	0.069	−0.597	6.4	2.7	90.9	0	69.5	3.8	26.5	0.2
	1	1	2	N.C.	Natural log	0.999	0.744	0.770	310.4, 15	0.000	−0.590								
	2	1	3	N.C.	Natural log	0.999	0.741	0.768	101.1, 13	0.000	−0.596								
S5	1	1	2	N.C.	Natural log	0.992	1.146	1.317	23.38, 15	0.076	0.273	40.1	0	59.9	0	76.1	3.4	18.8	1.7
	1	1	3	N.C.	Natural log	0.991	1.147	1.319	10.75, 14	0.070	0.275								
	2	1	3	N.C.	Natural log	0.991	1.147	1.319	9.66, 13	0.072	0.276								
S6	2	1	3	N.C.	Natural log	0.993	1.666	1.697	17.53, 13	0.176	1.020	88.0	0	12.0	0	57.9	1.6	35.9	4.6
	1	1	3	N.C.	Natural log	0.993	1.666	1.698	25.84, 14	0.027	1.021								
	1	1	2	N.C.	Natural log	0.993	1.665	1.700	58.99, 15	0.000	1.021								

Note.
[a] V: Vegetated (trees and grasslands); NV: Non-vegetated (bare soil); I: Impervious (roofs, pavements and footpaths); WB: Water body (rivers, lakes and wetlands).
[b] N.C.: Model without constant.
[c] RMSE: Root mean square error.
[d] MAPE: Mean absolute percentage error.
[e] BIC: Normalized Bayesian information criterion.

Table 4
Parameter estimates for the ARIMA model terms selected for PM_{10}.

Station (AR, I, MA)	Estimate		Standard error	*t* Ratio	Prob > |*t*|
S1 (2, 1, 2)	AR1	1.180	0.097	12.159	<0.001
	AR2	−0.284	0.077	−3.701	<0.001
	MA1	0.917	0.098	9.390	<0.001
	MA2	−0.148	0.055	−2.712	0.007
S2 (1, 1, 0)	AR1	0.012	0.004	2.724	0.006
	AR2	–	–	–	–
	MA1	–	–	–	–
	MA2	–	–	–	–
S3 (1, 1, 1)	AR1	0.745	0.071	10.440	<0.001
	AR2	–	–	–	–
	MA1	0.727	0.074	9.878	<0.001
	MA2	–	–	–	–
S4 (1, 1, 3)	AR1	0.866	0.005	63.878	<0.001
	AR2	–	–	–	–
	MA1	0.237	0.007	33.950	<0.001
	MA2	0.154	0.006	26.360	<0.001
	MA3	0.080	0.005	15.198	<0.001
S5 (1, 1, 2)	AR1	0.794	0.010	82.858	<0.001
	AR2	–	–	–	–
	MA1	0.556	0.011	52.273	<0.001
	MA2	0.042	0.006	7.292	<0.001
	MA3	–	–	–	–
S6 (2, 1, 3)	AR1	1.095	0.172	6.375	<0.001
	AR2	−0.209	0.140	−1.493	0.013
	MA1	0.856	0.172	4.980	<0.001
	MA2	−0.115	0.099	−1.163	<0.001
	MA3	0.019	0.009	1.968	0.005

results suggest that as monitoring station distances increase, the distribution of the impervious LSC becomes closer to uniform among monitoring stations (see Fig. 3). We chose S1 as the reference station for comparison with the ARIMA models developed for impervious LSC, and we chose 100 m as the distance of influence to analyze the possible differences among ARIMA models.

The results showed a difference among monitoring stations for the distribution of impervious LSC: 54.5% at S1, 93.0% at S2, and 91.2% at S3 (distance of influence = 100 m). Results for the autoregressive term (AR) of the ARIMA models likely suggest that these differences were associated with the LSC type. To reduce the impervious LSC around a monitoring station, an increase in the AR term of the ARIMA model was suggested (Table 3). Less impervious LSC around a monitoring station meant the PM_{10} concentrations of previous days had a greater effect. In this study, the effect or persistence of PM_{10} concentrations was 2 days or 48 h (S1 station, AR term = 2). Greater persistence of PM_{10} pollution was observed in urban areas with less impervious LSC (roofs, pavements, and footpaths) and more vegetated LSC (trees and grasslands). Díaz-Robles et al. (2008) and Taneja et al. (2016) reported that ARIMA models of order 1 and 2 in the AR term simulated daily PM concentrations in Temuco (Chile) and New Delhi (India), respectively.

A Spearman's correlation analysis for predominately vegetated LSC monitoring (S4, S5, and S6) showed that the monitoring station with the best correlations was, on average, S4 (37.0% of significant correlations, *p*-values < 0.05). Also, this analysis allowed us to observe the best and worst correlations for distances of influence of each monitoring station: 800 m (38.9% of significant correlations, *p*-values < 0.05) and 50 m (9.30% of significant correlations, *p*-values < 0.05), respectively. The reference station selected to compare the ARIMA models developed for vegetated LSC was S4, and the distance of influence selected to analyze the possible differences among ARIMA models was 50 m (Table 3).

Looking at the distribution of vegetated LSC, results showed a difference for monitoring stations: 6.4% at S4, 40.1% at S5, and 88.0% at S6 (distance of influence: 50 m). The AR term of the ARIMA models suggests a difference likely associated with vegetated LSC. To increase the vegetated LSC around a monitoring station would lead to an increase in the AR term of the ARIMA model developed (Table 3). It was observed that more vegetated LSC around a monitoring station resulted in a greater effect exerted by the previous days' PM_{10} concentrations. In this study the effect or persistence of PM_{10} concentrations was 2 days or 48 h (S6 station, AR term = 2), with results again suggesting a greater persistence in

PM_{10} pollution for urban areas with more vegetated LSC and less impervious LSC. These findings were consistent with those previously outlined for predominantly impervious LSC monitoring stations (S1, S2, and S3).

Together, these results suggest that PM_{10} concentrations in urban zones with predominantly vegetated LSC exhibit a longer-term background level, likely associated with lower levels of traffic intensity and industrial activity, than the studied urban zones with predominantly impervious LSC. Turias et al. (2008) reported a similar longer-term trend for PM concentrations in Gibraltar (Spain). As mentioned, urban zones classified as vegetated LSC areas registered lower concentrations of PM_{10} than urban zones classified as impervious LSC areas (average daily difference = 42.7%). Zou et al. (2016) stated that PM_{10} concentration variations were positively correlated with higher levels of built-up areas and negatively correlated with the forests of urban sprawls in China.

The moving average term (MA) of the ARIMA models demonstrated a difference that was likely associated with vegetated LSC. Results indicate that monitoring stations with predominantly vegetated LSC (S4, S5, and S6) registered a higher order of magnitude in the MA term (see Table 3). More vegetated LSC around a monitoring station meant a greater effect exerted by the previous days' PM_{10} variations. In this study, the effect was transmitted from 2 to 3 days immediately preceding measurement (MA term between 2 and 3). Consequently, results pointed to predominantly vegetated LSC areas as those exhibiting greater variability in PM_{10} concentrations. Additionally, these results suggest that in urban areas with predominantly impervious LSC (S1, S2, and S3), atmospheric pollutant sources likely had a more uniform trend in the emission cycles, as evidenced by less variability in PM_{10} concentrations (MA term between 0 and 2) than urban areas with predominantly vegetated LSC (S4, S5, and S6). On this matter, Fig. 4b shows the measured and simulated values (24-h moving average) of a day selected at random (date: 12/04/2009).

4. Conclusions

In this study, we use ARIMA models for daily temporal analysis (over a 6-year range, 2007–2012) of the effect of LSC on PM_{10} concentrations in a high-altitude megacity, Bogota. This study's findings allow us to draw the following conclusions.

ARIMA analyses suggest a greater persistence of PM_{10} pollution in the presence of more vegetated LSC (trees and grasslands); this same factor decreases in the presence of more impervious LSC (roofs, pavements and footpaths). In this study, the persistence of PM_{10} pollution in urban areas with predominantly vegetated LSC is 2 days (48 h). This is shown by an increase in the AR term of the ARIMA models used herein. As for the MA term, this tends to increase in urban areas with predominantly vegetated LSC. Results suggest that in these areas, PM_{10} concentrations are more variable. The best distance to demonstrate these findings is between 50 and 100 m relative to the physical location of PM_{10} monitoring stations. Urban areas with a predominantly vegetated LSC register lower PM_{10} concentrations than urban areas with predominantly impervious LSC (average daily difference = 42.7%).

Finally, the findings of this research serve as a reference point from which researchers can expand the body of knowledge regarding the application and interpretation of ARIMA models in PM_{10} studies, namely for the development and implementation of differentiated strategies for air pollution control germane to urban LSC. However, the following limitations form part of this study and require further attention. First, the number of years for the PM_{10} time series (6 years) is not longer because of LSC changes in the areas covered by the monitoring stations; for ARIMA analysis, the same LSC distribution is required throughout the entirety of the study period. Second, the monitoring stations do not have similar characteristics with regard to the location distance and emission intensity of the PM_{10} sources (highways and industries). Third, AS for the entire research area is evaluated using data from three monitoring stations of a total of six monitoring stations used in this study.

Conflict of interest

The authors declare that there are no conflicts of interest.

Acknowledgment

The authors wish to thank the University 'Francisco José de Caldas' (Colombia) and Environment Secretary of Bogota (Colombia) for their financial support. Special thanks are due to Mr. Joseph Wager who revised the English version of this paper. Finally, the authors are very grateful for the helpful comments and suggestions offered by reviewers.

References

Argiriou, A.A., 2007. Use of neural networks for tropospheric ozone time series approximation and forecasting-A review. Atmos. Chem. Phys. Discuss. 7, 5739–5767.

Athanasiadis, I.N., Karatzas, K., Mitkas, P., 2005. Contemporary air quality forecasting methods: a comparative analysis between classification algorithms and statistical methods. In: Fifth International Conference on Urban Air Quality Measurement, Modelling and Management, March 29-31, 2005, Valencia, Spain, pp. 1–12.

Avecilla, F., Panebianco, J.E., Buschiazzo, D.E., 2016. A wind-tunnel study on saltation and PM_{10} emission from agricultural soils. Aeolian Res. 22, 73–83.

Bach, P.M., Staalesen, S., McCarthy, D.T., Deletic, A., 2015. Revisiting land use classification and spatial aggregation for modelling integrated urban water systems. Landsc. Urban Plann 143, 43–55.

Bathmanabhan, S., Saragur Madanayak, S.N., 2010. Analysis and interpretation of particulate matter - PM_{10}, $PM_{2.5}$ and PM_1 emissions from the heterogeneous traffic near an urban roadway. Atmos. Pollut. Res. 1, 184–194.

Box, G.E.P., Jenkins, G.M., 1970. Time Series Analysis, Forecasting and Control, first ed. Holden-Day, San Francisco.

Carvacho, O.F., Ashbaugh, L.L., Brown, M.S., Flocchini, R.G., 2004. Measurement of $PM_{2.5}$ Emission Potential from Soil Using the UC Davis Resuspension Test Chamber. Geomorphology 59, 75–80.

Chambers, S.D., Wang, F., Williams, A.G., Xiaodong, D., Zhang, H., Lonati, G., Crawford, J., Griffiths, A.D., Ianniello, A., Allegrini, I., 2015. Quantifying the influences of atmospheric stability on air pollution in Lanzhou, China, using a radon-based stability monitor. Atmos. Environ. 107, 233–243.

Chen, X., Pei, T., Zhou, Z., Teng, M., He, L., Luo, M., Liu, X., 2015. Efficiency differences of roadside greenbelts with three configurations in removing coarse particles (PM_{10}): a street scale investigation in Wuhan, China. Urban For. Urban Gree 14, 354–360.

Chow, J.C., Watson, J.G., Mauderly, J.L., Costa, D.L., Wyzga, R.E., Vedal, S., Hidy, G.M., Altshuler, S.L., Marrack, D., Heuss, J.M., Wolff, G.T., Pope, C.A., Dockery, D.W., 2006. Health effects of fine particulate air pollution: lines that connect. Japca J. Air Waste Ma 56, 1368–1380.

Connell, D.P., Withum, J.A., Winter, S.E., Statnick, R.M., Bilonick, R.A., 2005. The Steubenville Comprehensive Air Monitoring Program (SCAMP): analysis of short-term and episodic variations in $PM_{2.5}$ concentrations using hourly air monitoring data. Japca J. Air Waste Ma 55, 559–573.

Díaz-Robles, L.A., Ortega, J.C., Fu, J.S., Reed, G.D., Chow, J.C., Watson, J.G., Moncada-Herrera, J.A., 2008. A hybrid ARIMA and artificial neural networks model to forecast particulate matter in urban areas: the case of Temuco, Chile. Atmos. Environ. 42, 8331–8340.

Fowler, D., Skiba, U., Nemitz, E., Choubedar, F., Branford, D., Donovan, R., Rowland, P., 2004. Measuring aerosol and heavy metal deposition on urban woodland and grass using inventories of 210PB and metal concentrations in soil. Water Air Soil Pollut. Focus 4, 483–499.

Funk, R., Reuter, H.I., Hoffmann, C., Engel, W., Öttl, D., 2008. Effect of moisture on fine dust emission from tillage operations on agricultural soils. Earth Surf. Process. Landf. 33, 1851–1863.

Gallagher, M.W., Nemitz, E., Dorsey, J.R., Fowler, D., Sutton, M.A., Flynn, M., Duyzer, J., 2002. Measurements and parameterizations of small aerosol deposition velocities to grassland, arable crops, and forest: influence of surface roughness length on deposition. J. Geophys. Res. D. Atmos. 107 (D12, 10) http://dx.doi.org/10.1029/2001JD000817 issn:0148–0227.

Gifford, F.A., 1976. Turbulent diffusion typing schemes: a review. Nucl. Saf. 17, 68–86.

Gocheva-Ilieva, S.G., Ivanov, A.V., Voynikova, D.S., Boyadzhiev, D.T., 2014. Time series analysis and forecasting for air pollution in small urban area: an SARIMA and factor analysis approach. Stoch. Environ. Res. Risk Assess. 28, 1045–1060.
Gomišček, B., Hauck, H., Stopper, S., Preining, O., 2004. Spatial and temporal variations of PM_1, $PM_{2.5}$, PM_{10} and particle number concentration during the AUPHEP – project. Atmos. Environ. 38, 3917–3934.
Hernández, E., Martín, F., Valero, F., 1992. Statistical forecast models for daily air particulate iron and lead concentrations for Madrid. Spain. Atmos. Environ. Part B Urban Atmos. 26, 107–116.
Hsu, H., Adamkiewicz, G., Houseman, E.A., Spengler, J.D., Levy, J.I., 2014. Using mobile monitoring to characterize roadway and aircraft contributions to ultrafine particle concentrations near a mid-sized airport. Atmos. Environ. 89, 688–695.
Irga, P.J., Burchett, M.D., Torpy, F.R., 2015. Does urban forestry have a quantitative effect on ambient air quality in an urban environment? Atmos. Environ. 120, 173–181.
Islam, M.N., Rahmanb, K.S., Bahar, M.M., Habib, M.A., Andoa, K., Hattoria, N., 2012. Pollution attenuation by roadside greenbelt in and around urban areas. Urban For. Urban Gree 11, 460–464.
Jian, L., Zhao, Y., Zhu, Y., Zhang, M., Bertolatti, D., 2012. An application of ARIMA model to predict submicron particle concentrations from meteorological factors at a busy roadside in Hangzhou, China. Sci. Total Environ. 426, 336–345.
Kumar, U., De Ridder, K., 2010. GARCH modelling in association with FFT-ARIMA to forecast ozone episodes. Atmos. Environ. 44, 4252–4265.
Kumar, U., Jain, V.K., 2010. ARIMA forecasting of ambient air pollutants (O_3, NO, NO_2 and CO). Stoch. Environ. Res. Risk Assess. 24, 751–760.
Lee, S., Ho, C., Lee, Y.G., Choi, H., Song, C., 2013. Influence of transboundary air pollutants from China on the high-PM_{10} episode in Seoul. Korea for the period October 16-20, 2008 Atmos. Environ. 77, 430–439.
Liu, J., Mo, L., Zhu, L., Yang, Y., Liu, J., Qiu, D., Zhang, Z., Liu, J., 2016. Removal efficiency of particulate matters at different underlying surfaces in Beijing. Environ. Sci. Pollut. Res. 23, 408–417.
Liu, P.G., 2009. Simulation of the daily average PM_{10} concentrations at Ta-Liao with Box-Jenkins time series models and multivariate analysis. Atmos. Environ. 43, 2104–2113.
Ljung, G.M., Box, G.E.P., 1978. On a measure of a lack of fit in time series models. Biometrika 65, 297–303.
Meraz, M., Rodriguez, E., Femat, R., Echeverria, J.C., Alvarez-Ramirez, J., 2015. Statistical persistence of air pollutants (O_3, SO_2, NO_2 and PM_{10}) in Mexico City. Phys. A Stat. Mech. Appl. 427, 202–217.
McDonald, A.G., Bealey, W.J., Fowler, D., Dragosits, U., Skiba, U., Smith, R.I., Donovan, R.G., Brett, H.E., Hewitt, C.N., Nemitz, E., 2007. Quantifying the effect of urban tree planting on concentrations and depositions of PM_{10} in two UK conurbations. Atmos. Environ. 41, 8455–8467.
Minguillon, M.C., Querol, X., Baltensperger, U., Prevot, A.S.H., 2012. Fine and coarse PM composition and sources in rural and urban sites in Switzerland: local or regional pollution? Sci. Total Environ. 427, 191–202.
Montoya, G.J., Cepeda, W., Eslava, J.A., 2004. Características de la turbulencia y de la estabilidad atmosférica en Bogotá. Rev. Acad. Colomb. Cienc. 28, 327–335.
Nelson, G., Maisonet, M., Miyashiro, M., 2005. An Assessment of Health Effects of Ambient Air Pollution in Latin America and the Caribbean, first ed. Pan Americana Health Organization, Washington D.C.
Pasquill, F., 1961. The estimation of the dispersion of windborne material. Meteorol. Mag. 90, 33–49.
Perrino, C., Catrambone, M., Pietrodangelo, A., 2008. Influence of atmospheric stability on the mass concentration and chemical composition of atmospheric particles: a case study in Rome, Italy. Environ. Int. 34, 621–628.
Pope, C.A., Dockery, D.W., 2006. Health effects of fine particulate air pollution: lines that connect. Japca J. Air Waste Ma 56, 709–742.
Reisen, V.A., Sarnaglia, A.J.Q., Reis, N.C., Lévy-Leduc, C., Santos, J.M., 2014. Modeling and forecasting daily average PM_{10} concentrations by a seasonal long-memory model with volatility. Environ. Model. Softw. 51, 286–295.
Sarmiento, R., Hernández, L.J., Medina, E.K., Rodríguez, N., Reyes, J., 2015. Respiratory symptoms associated with air pollution in five localities of Bogotá, 2008-2011, a dynamic cohort study. Biomedica 35, 167–176.
Schwarz, G., 1978. Estimating the dimension of a model. Ann. Stat. 6, 461–464.
Seinfeld, J., Pandis, S., 2016. Atmospheric Chemistry and Physics: from Air Pollution to Climate Change, third ed. John Wiley & Sons, New Jersey.
Soni, K., Kapoor, S., Parmar, K.S., Kaskaoutis, D.G., 2014. Statistical analysis of aerosols over the Gangetic-Himalayan region using ARIMA model based on long-term MODIS observations. Atmos. Res. 149, 174–192.
Soto, D.F.P., Mejía, C.A.Z., Miranda, J.P.R., 2014. Evaluation of the air quality by using a mobile laboratory: Puente Aranda (Bogotá D.C., Colombia). Rev. Fac. Ing. 71, 153–166.
Sun, L., Wei, J., Duan, D.H., Guo, Y.M., Yang, D.X., Jia, C., Mi, X.T., 2016. Impact of Land-Use and Land-Cover Change on urban air quality in representative cities of China. J. Atmos. Sol–Terr. Phys. 142, 43–54.
Taneja, K., Ahmad, S., Ahmad, K., Attri, S., 2016. Time series analysis of aerosol optical depth over New Delhi using Box–Jenkins ARIMA modeling approach. Atmos. Pollut. Res. 7, 585–596.
Titos, G., Lyamani, H., Pandolfi, M., Alastuey, A., Alados-Arboledas, L., 2014. Identification of fine (PM_1) and coarse (PM_{10-1}) sources of particulate matter in an urban environment. Atmos. Environ. 89, 593–602.
Turias, I.J., González, F.J., Martin, M.L., Galindo, P.L., 2008. Prediction models of CO, SPM and SO_2 concentrations in the Campo de Gibraltar Region, Spain: a multiple comparison strategy. Environ. Monit. Assess. 143, 131–146.
Turner, D.B., 1964. A diffusion model for an urban area. J. Appl. Meteorol. 3, 83–91.
U.S.EPA (Environmental Protection Agency), 1999. Compendium of Methods for the Determination of Inorganic Compounds in Ambient Air. U.S.EPA/625/R-96/010a, Washington D.C., p. 723.
Vecchi, R., Marcazzan, G., Valli, G., 2007. A study on nighttime-daytime PM_{10} concentration and elemental composition in relation to atmospheric dispersion in the urban area of Milan (Italy). Atmos. Environ. 41, 2136–2144.
Waked, A., Favez, O., Alleman, L.Y., Piot, C., Petit, J.E., Delaunay, T., Verlinden, E., Golly, B., Besombes, J.L., Jaffrezo, J.L., Leoz-Garziandia, E., 2014. Source apportionment of PM_{10} in a north-western Europe regional urban background site (Lens, France) using positive matrix factorization and including primary biogenic emissions. Atmos. Chem. Phys. 14, 3325–3346.
Wang, P., Liu, Y., Qin, Z., Zhang, G., 2015. A novel hybrid forecasting model for PM_{10} and SO_2 daily concentrations. Sci. Total Environ. 505, 1202–1212.
Wolf-Benning, U., Draheim, T., Endlicher, W., 2009. Spatial and temporal differences of particulate matter in Berlin. Int. J. Environ. Waste Manag. 4, 3–16.
Yin, S., Cai, J.P., Chen, L.P., Shen, Z.M., Zou, X.D., Wu, D., Wang, W.H., 2007. Effects of vegetation status in urban green spaces on particle removal in a street canyon atmosphere. Acta Ecol. Sin. 27, 4590–4595.
Zhang, H., Liu, Y., Shi, R., Yao, Q., 2013. Evaluation of PM_{10} forecasting based on the artificial neural network model and intake fraction in an urban area: a case study in Taiyuan City, China. J. Air Waste Manag. Assoc. 63, 755–763.
Zhang, Y., Bocquet, M., Mallet, V., Seigneur, C., Baklanov, A., 2012. Real-time air quality forecasting, part I: history, techniques, and current status. Atmos. Environ. 60, 632–655.
Zhou, Q., Jiang, H., Wang, J., Zhou, J., 2014. A hybrid model for $PM_{2.5}$ forecasting based on ensemble empirical mode decomposition and a general regression neural network. Sci. Total Environ. 496, 264–274.
Zoras, S., Triantafyllou, A.G., Deligiorgi, D., 2006. Atmospheric stability and PM_{10} concentrations at far distance from elevated point sources in complex terrain: worst-case episode study. J. Environ. Manag. 80, 295–302.
Zou, B., Xu, S., Sternberg, T., Fang, X., 2016. Effect of land use and cover change on air quality in urban sprawl. Sustain. Switz. 8 http://dx.doi.org/10.3390/su8070677.